ReGeo
ISSN: 2177-3246

HYDRODYNAMIC CHARACTERIZATION OF MARAJÓ BAY WITHIN THE AREA OF INFLUENCE OF THE BARCARENA INDUSTRIAL DISTRICT

CARACTERIZAÇÃO HIDRODINÂMICA DA BAÍA DE MARAJÓ NA ÁREA DE INFLUÊNCIA DO DISTRITO INDUSTRIAL DE BARCARENA

CARACTERIZACIÓN HIDRODINÁMICA DE LA BAHÍA DE MARAJÓ EN LA ZONA DE INFLUENCIA DEL DISTRITO INDUSTRIAL DE BARCARENA

https://doi.org/10.56238/revgeov17n11-036

Data de submissão: 06/10/2026 **Data de publicação:** 06/11/2026

Sabrina Borges Lopes Pantoja[1], Gundisalvo Piratoba Morales[2], Paulo Cesar Colonna Rosman[3], Monica Frickmann Young Buckmann[4], Verônica Silveira de Andrade[5]

ABSTRACT

The hydrodynamic characterization of Marajó Bay was conducted through computational modeling using SisBaHiA®, aiming to identify tidal types and amplitudes, flood and ebb slack waters, high and low tides, the relationship between flow velocity and water level elevation, and phase differences. The hydrodynamic characteristics of this estuarine system are influenced by astronomical forcings, local environmental features, bathymetry, bottom shear stress, morphology, and river discharge. Methodological activities included the definition of the modeling domain, finite element mesh discretization, and 2DH hydrodynamic modeling. To identify fluvial and marine influences on the hydrodynamic behavior of Marajó Bay, five control stations were established along an area extending in the NE-SW direction. The simulated scenarios corresponded to the periods of highest and lowest rainfall in the region for the year 2021 (March and October, respectively). The results demonstrate that the region presents a predominantly stationary semi-diurnal tide, with phase differences and ebb durations increasing upstream of the modeling domain. Maximum velocities did not exceed 1.15 m/s. The hydrodynamic patterns identified in the study area are of paramount importance and can be utilized to assess potential environmental impacts in the aquatic system caused by the discharge of industrial effluents from the Barcarena Industrial District (DIB) or sanitary sewage from communities and urban centers located along the margins of this vital water system in Northern Brazil.

Keywords: Characterization. DIB. Hydrodynamics. Propagation. Types Tides.

[1] PhD Candidate in Environmental Sciences. Programa de Pós-Graduação em Ciências Ambientais (PPGCA). Universidade Estadual do Pará (UEPA). E-mail: sabrinaborges1404@gmail.com Orcid: 0009-0006-5057-8507
[2] Professor Dr. Programa de Pós-Graduação em Ciências Ambientais (PPGCA). Universidade Estadual do Pará (UEPA). E-mail: gundisalvo.morales@uepa.br Orcid: 0000-0002-5930-7053
[3] Professor Dr. Universidade Federal do Rio de Janeiro (URFJ). E-mail: pccrosman@ufrj.br Orcid: 0000-0001-7687-0959
[4] Research Engineer – Coastal and Oceanographic Engineering Field. Universidade Federal do Rio de Janeiro (URFJ). E-mail: myoung@oceanica.ufrj.br Orcid: 0000-0002-7439-356X
[5] PhD candidate.Instituto Alberto Luiz Coimbra de Pós-Graduação e Pesquisa de Engenharia (COPPE). Universidade Federal do Rio de Janeiro (URFJ). E-mail: veronicasilveiraandrade@gmail.com Orcid: 0000-0001-9025-874X

RESUMO
Foi realizada a caracterização hidrodinâmica da Baia de Marajó através de modelagem computacional utilizando o SisBaHiA®, visando identificar amplitude tipo e regime da maré, estofas de enchente e vazante, preamar e baixa-mar, relação da velocidade com a elevação do nível da água e estofas e diferença de fases. As características hidrodinâmicas, deste sistema estuarino, estão influenciadas pelas forçantes astronômicas, as características ambientais locais, a batimetria, tensão de fundo, morfologia e vazões fluviais. As atividades realizadas incluíram a definição do domínio de modelagem, discretização de malha de elementos finitos e modelagem hidrodinâmica 2DH. Visando identificar a influência fluvial e marinha nas características hidrodinâmicas da Baia de Marajó, foram estabelecidas 5 estações de controle ao longo da área que se estende em direção NE-SW. Os cenários simulados foram e época de maior e menor pluviosidade da região no ano de 2021, e que correspondem ao mês de março e outubro respectivamente. Os resultados mostram que a região apresenta maré semidiurna predominantemente do tipo estacionária, com diferença de fases e tempos de vazante aumentando no sentido montante do domino de modelagem, com velocidades máximas que não ultrapassaram 1.15 m/s. As características hidrodinâmicas encontradas na área de estudo são de grande importância, e poderão ser utilizados para dimensionar possíveis impactos ambientais causados, no sistema hídrico, pelo lançamento de efluentes indústrias provenientes do Distrito Industria de Barcarena-DIB, ou efluentes sanitários das comunidades e centros urbanos alocados nas margens deste importante sistema hídrico da região norte do Brasil.

Palavras-chave: Caracterização. DIB. Hidrodinâmica. Tipos de Marés. Propagação.

RESUMEN
La caracterización hidrodinámica de la Bahía de Marajó se realizó mediante modelado computacional con SisBaHiA®, con el objetivo de identificar la amplitud y el régimen de mareas, las mareas altas y bajas, la relación entre la velocidad y el aumento del nivel del agua, y las mareas y las diferencias de fase. Las características hidrodinámicas de este sistema estuarino están influenciadas por forzamientos astronómicos, características ambientales locales, batimetría, tensión del fondo, morfología y caudales fluviales. Las actividades realizadas incluyeron la definición del dominio de modelado, la discretización de la malla de elementos finitos y el modelado hidrodinámico 2DH. Para identificar la influencia fluvial y marina en las características hidrodinámicas de la Bahía de Marajó, se establecieron 5 estaciones de control a lo largo del área, extendiéndose en dirección NE-SO. Los escenarios simulados correspondieron a los periodos de mayor y menor precipitación en la región durante 2021, correspondientes a los meses de marzo y octubre, respectivamente. Los resultados muestran que la región presenta una marea semidiurna predominantemente estacionaria, con diferencias de fase y tiempos de reflujo que aumentan aguas arriba del dominó modelado, con velocidades máximas que no superaron 1,15 m/s. Las características hidrodinámicas encontradas en el área de estudio son de gran importancia y pueden utilizarse para evaluar posibles impactos ambientales causados en el sistema hídrico por la descarga de efluentes industriales del Distrito Industrial de Barcarena (DIB), o efluentes sanitarios de comunidades y centros urbanos ubicados en las riberas de este importante sistema hídrico en la región norte de Brasil.

Palabras clave: Caracterización. DIB. Hidrodinámica. Tipos de Marea. Propagación.

1 INTRODUCTION

The Barcarena Industrial District (DIB), located on the right bank of the Pará River, is an integral part of Marajó Bay. It accommodates companies from various sectors, most notably those involved in kaolin and alumina processing, aluminum cable production, fertilizers, and cargo transportation. According to CODEC (2018), the DIB comprises approximately 90 companies whose industrial activities primarily focus on mining and services.

The Pará River, embedded within the Marajó Bay water system, serves as a receiving body for the dilution, dispersion, and self-purification of industrial effluents from the DIB and domestic sewage from the populations situated along its banks. From a regulatory perspective, much of the Marajó Bay water system is classified as freshwater under CONAMA Resolution 357/2005 (CONAMA, 2005). Furthermore, all discharged effluents must comply with the requirements of CONAMA Resolution 430/2011 (CONAMA, 2011), which establishes the conditions and standards for effluent discharge.

The expansion of the DIB since its establishment in 1979 contrasts sharply with a history of environmental accidents, primarily caused by the leakage of industrial effluents. These incidents stem from both unidentified diffuse sources – such as the soot emission in 2004 and the 2008 contamination of Caripi Beach – and identified point sources, notably the 2007 leakage of approximately 300,000 m³ of kaolin effluent into the Curuperé and Dendê streams. According to Nascimento and Silva (2021), approximately 24 environmental accidents occurred in the DIB between 2001 and 2021. Characterized as “socio-ethnic and environmental disasters,” these events have been denounced by local communities and documented by environmental agencies, inspection bodies, and specialized literature (IEC, 2018; Pereira *et al.*, 2007; Castro and Carmo, 2019).

Despite the frequency of these accidents, no comprehensive regional or local studies have been conducted to determine the behavior of contamination plumes by analyzing the hydrodynamic characteristics of the affected water bodies. Such studies are vital for implementing corrective or preventive measures proportionate to the magnitude of each incident. In-depth research considering hydrodynamics and advective-diffusive transport (both Eulerian and Lagrangian) is essential and can be executed using advanced modeling tools, such as the Environmental Hydrodynamics Base System (SisBaHiA®) (Rosman, 2012, 2021).

In this context, the present study provides an environmental hydrodynamic analysis of Marajó Bay within the DIB's area of influence. The investigation includes digital terrain modeling and the hydrodynamic characterization of the water system using SisBaHiA®. These hydrodynamic models serve as a foundation for future simulations of the spatio-temporal behavior of effluents that may eventually be released into the region, supporting more effective environmental management (Gallo, 2009; Barros, 2012; Lima Neto *et al*., 2021).

2 MATERIALS AND METHODS

This section details the study area and the applied methodology, which encompasses digital terrain modeling and hydrodynamic modeling. The environmental data utilized in each stage are also discussed.

2.1 STUDY AREA

The study area comprises the estuarine system formed by the Guajará and Marajó Bays, which accommodate the Metropolitan Region of Belém and the Barcarena Industrial District (DIB). The latter encompasses 24 of the 143 municipalities in the state of Pará. This region serves as a transition zone between fresh and brackish water – predominantly fresh – characterized by a prevalence of cohesive muddy sediments. The DIB is situated in the municipality of Barcarena, on the right bank of the Pará River within Marajó Bay. Other significant tributaries of this bay include the Guamá, Pará, Capim, Acará, Tocantins, and Moju Rivers. The primary urban and industrial centers of the state of Pará are located along the banks of Marajó Bay (Figure 1).

2.2 COMPUTATIONAL MODELS

Computational simulations were conducted using the Environmental Hydrodynamics Base System (SisBaHiA®). This is a well-established professional computational system developed at the Alberto Luiz Coimbra Institute for Graduate Studies and Engineering Research of the Federal University of Rio de Janeiro (COPPE/UFRJ). SisBaHiA® is extensively applied in research, engineering projects, and environmental management of water resources. The models implemented within the system are designed to predict water circulation and the transport of scalar quantities, suitable for scenario simulations in coastal waters, bays, estuaries, rivers, canals, reservoirs, lakes, and lagoons (Rosman, 2021).

For the purposes of this study, a vertically integrated two-dimensional (2DH) hydrodynamic model was employed. These models are optimized for natural water bodies where variable density effects can be neglected. All hydrodynamic and environmental modeling activities were performed using SisBaHiA® version 11, which has been continuously refined at COPPE/UFRJ since 1987 (Rosman, 2021).

In a given time interval, the model calculates the vertically averaged velocity components in the x and y directions, $U(x,y,t)$ and $V(x,y,t)$ respectively, as well as the free surface elevations, $z = \zeta (x,y,t)$. These calculations are based on the continuity equation and the **momentum equations** in the x and y directions (Rosman, 2021). Equation 1 presents the governing hydrodynamic equations for the 2DH model in the x-direction, while Equation 2 presents the momentum equation for a vertically integrated flow in the y-direction.

Figure 1

Area of study.

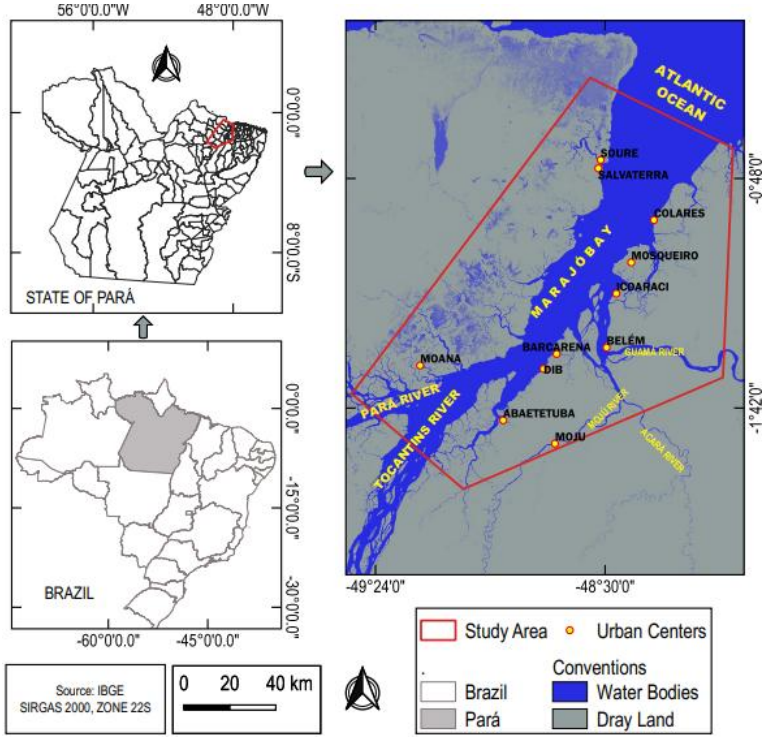

Source: Prepared by the authors themselves.

$$\frac{\partial U}{\partial t} + U\frac{\partial U}{\partial x} + V\frac{\partial U}{\partial y} = -g\frac{\partial \zeta}{\partial x} - g\frac{(\zeta+h)}{2}\frac{\partial(\hat{\rho}/\rho_0)}{\partial x} + \frac{1}{\rho_0(\zeta+h)}\left(\frac{\partial[(\zeta+h)\widehat{\tau_{xx}}]}{\partial x} + \frac{\partial[(\zeta+h)\widehat{\tau_{xy}}]}{\partial y}\right) + \frac{1}{\rho_0(\zeta+h)}(\tau_x^S - \tau_x^B - \tau_x^E) - \frac{1}{\rho_0(\zeta+h)}\left(\frac{\partial S_{xx}}{\partial x} + \frac{\partial S_{xy}}{\partial y}\right) + 2\Omega \sin\Phi V - \frac{U}{\zeta+h}\sum q$$

(1)

$$\frac{\partial V}{\partial t} + U\frac{\partial V}{\partial x} + V\frac{\partial V}{\partial y} = -g\frac{\partial \zeta}{\partial y} - g\frac{(\zeta+h)}{2}\frac{\partial(\hat{\rho}/\rho_0)}{\partial y} + \frac{1}{\rho_0(\zeta+h)}\left(\frac{\partial[(\zeta+h)\widehat{\tau_{xy}}]}{\partial x} + \frac{\partial[(\zeta+h)\widehat{\tau_{yy}}]}{\partial y}\right) + \frac{1}{\rho_0(\zeta+h)}(\tau_y^S - \tau_y^B - \tau_y^E) - \frac{1}{\rho_0(\zeta+h)}\left(\frac{\partial S_{yx}}{\partial x} + \frac{\partial S_{yy}}{\partial y}\right) - 2\Omega \sin\Phi U - \frac{V}{(\zeta+h)}\sum q$$

(2)

The Equation of continuity (of the volume) integrated along the vertical is presented in Equation 3.

$$\frac{\partial(\zeta+h)}{\partial t} + \frac{\partial UH}{\partial x} + \frac{\partial VH}{\partial y} = \sum q \qquad (3)$$

2.3 DIGITAL TERRAIN MODELING (DTM)

The DTM involves defining the modeling domain, discretizing this domain into a computational mesh, and incorporating bathymetric data and equivalent bottom roughness.

- Definition of the Domain of Interest

The domain boundaries are categorized into two types: open boundaries with free flow and land boundaries (terrestrial contours), which represent the bay shores, islands, and sections of rivers or canals (Rosman, 2021). For Marajó Bay, the boundaries were delimited using Google Earth imagery and refined using Surfer® software. The resulting land and water contour files were utilized to define the finite element mesh within SisBaHiA®. Figure 2 (a) illustrates the domain of interest.

- Mesh Discretization

The generated finite element mesh comprises a total of 1,424 elements, consisting of 1,283 quadrangular and 141 triangular elements. The mesh includes 6,253 calculation nodes, categorized into 4,519 internal nodes, 1,705 land boundary nodes, and 31 open boundary nodes (Figure 2 (a)).

- Bathymetry Data

Bathymetric data for Guajará Bay, Marajó Bay, and the Pará River were obtained from nautical charts 302, 303, 304, 305, 306, 320, and 321, provided by the Directorate of Hydrography and Navigation (DHN) of the Brazilian Navy. The bathymetric data were compiled, organized, and subsequently interpolated using the Kriging method in Surfer® software. The resulting grid was then mapped onto the SisBaHiA® mesh. Figure 2 (b) presents the interpolated bathymetry utilized in this study.

Figure 2

Model domain and spatial discretization: (a) Study area mesh and base map; (b) Interpolated bathymetry and locations of the meteorological (wind) stations.

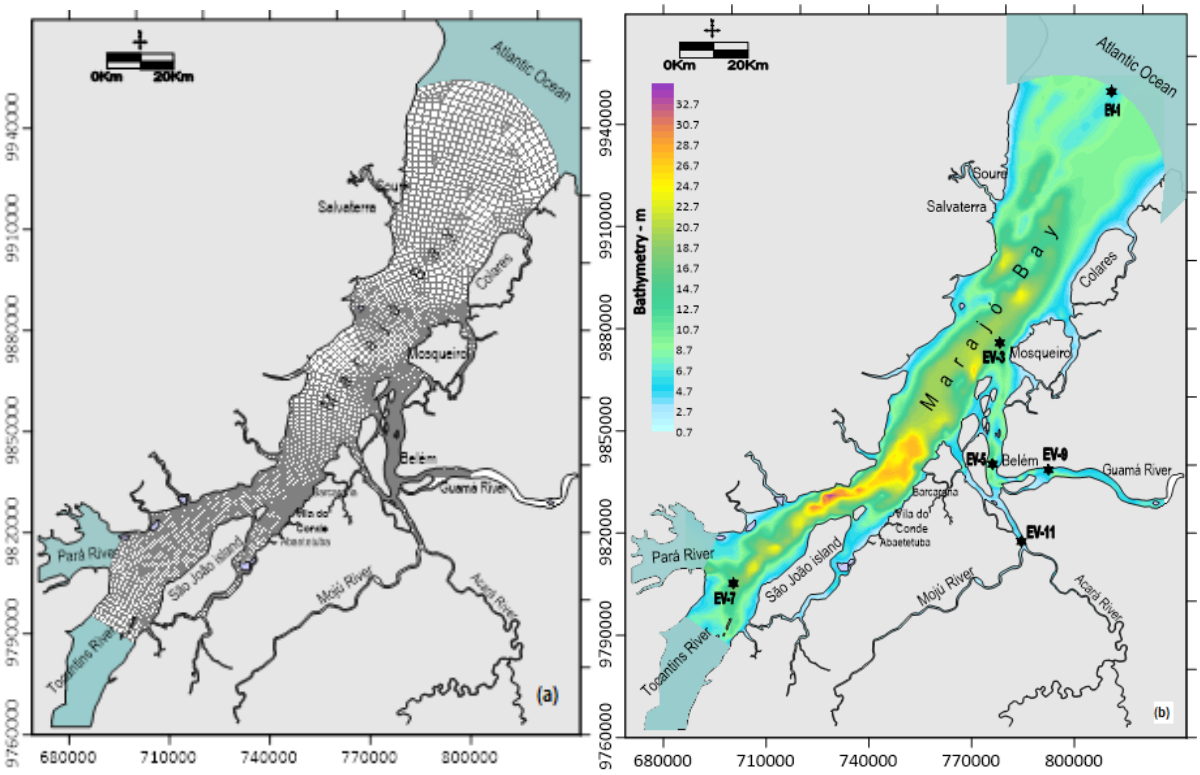

Source: Prepared by the authors themselves.

2.4 HYDRODYNAMIC MODELING

This section presents the adopted modeling scenarios and the boundary conditions used to characterize them.

2.4.1 Scenarios

The modeling was conducted for two distinct seasonal periods: the rainy season and the dry season. The rainy season is represented by the month of March, while the dry season is represented by October.

2.4.2 Environmental data and boundary conditions

To characterize these scenarios, data regarding winds, astronomical tides, and river discharges were incorporated as detailed below.

- Wind Data

Wind information was obtained from the ERA5 hourly reanalysis data on single levels (from 1979 to the present), available through the Copernicus Climate Data Store. Figure 3 illustrates the locations of the six wind stations utilized. Wind speed and direction were derived from the velocity components (U and V) and converted into magnitude and azimuthal direction for integration into the models. In the study region, the predominant wind directions during the rainy season are NE, ENE, and N. A similar pattern is observed during the dry season, with prevailing NE and ENE directions (Figure 3).

Figure 3

Wind roses at Station 5: (a) Rainy season and (b) Dry season.

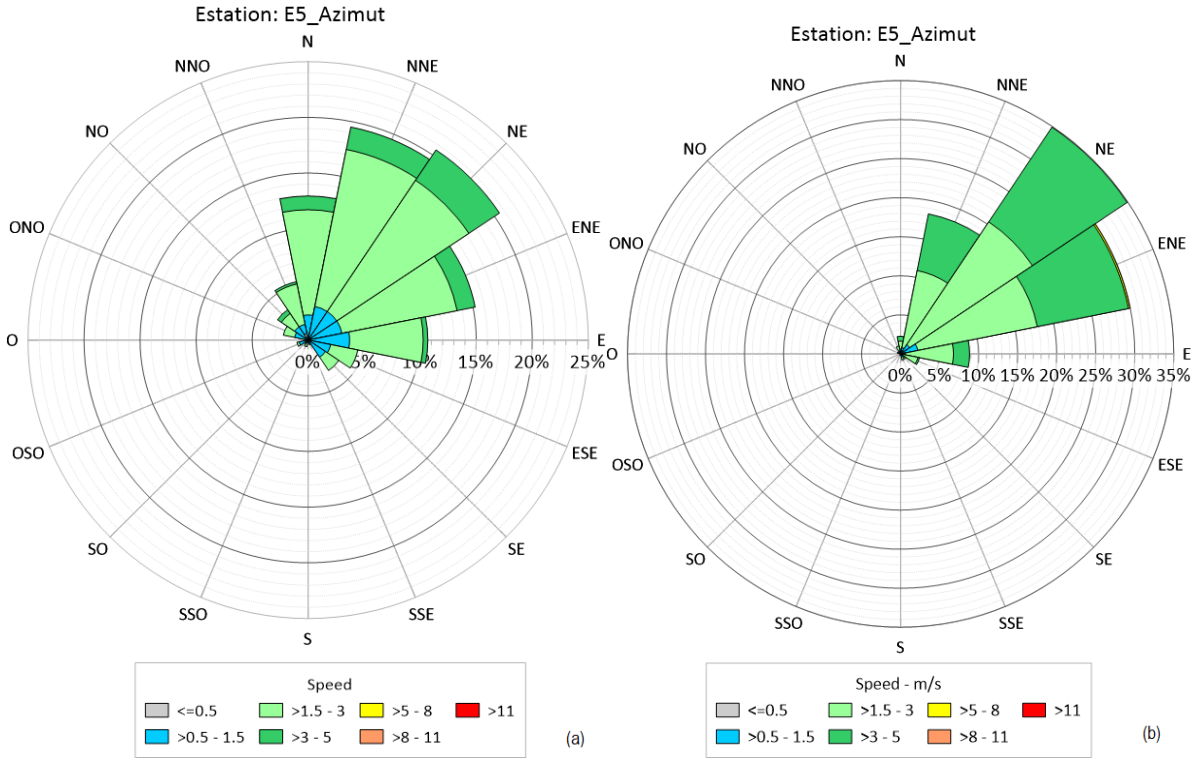

Source: Prepared by the authors themselves.

- Astronomical Tide Data

To characterize the astronomical tide in Marajó Bay, 33 harmonic constants obtained from the FES2014 (Finite Element Solution, 2014) global tide model were applied at an open boundary point at the entrance of Marajó Bay (Table 1). Based on these harmonic constants, the model calculates the time series of free surface elevations for each node along the open boundary.

It is important to note that tidal propagation is significantly influenced by ocean bathymetry and, more critically, by the specific geometry of bays and estuaries. As the tide enters these systems, tidal forces are modified by local dynamic forces, such as bottom friction and morphological constraints. While the frequencies of the tidal constituents remain unchanged, their amplitudes and phases vary according to the specific location within the estuary.

Table 1

Tidal harmonic constituents used for the open boundary condition.

Constant	Period (sec)	Amplitude (m)	Phase (grey)	Energy	Accumulated En.	% Accumulated En.
M2	44714.16431	1.50841	243.38458	2.27531	2.27531	86.53
S2	43200.00002	0.42816	278.97974	0.18332	2.45863	93.50
N2	45570.05357	0.30107	231.96257	0.09064	2.54927	96.94
K2	43082.04529	0.13590	276.32977	0.01847	2.56774	97.65
K1	86164.09058	0.10461	258.73309	0.01094	2.57869	98.06
M6	14904.72144	0.09902	154.91881	0.00980	2.58849	98.44
O1	92949.63010	0.08943	235.41574	0.00800	2.59649	98.74
L2	43889.83274	0.07759	250.75989	0.00602	2.60251	98.97
MS4	21972.02139	0.07484	99.25659	0.00560	2.60811	99.18
nu2	45453.61584	0.06453	222.24214	0.00416	2.61227	99.34
MSf	1275721.42300	0.05912	26.16555	0.00350	2.61577	99.47
MN4	22569.02603	0.05663	38.41562	0.00321	2.61897	99.59
M4	22357.08217	0.04467	150.37077	0.00200	2.62097	99.67
mu2	46338.32735	0.04100	289.82590	0.00168	2.62265	99.73
Mm	2380713.36500	0.03825	21.55040	0.00146	2.62411	99.79
2N2	46459.34794	0.03791	221.05270	0.00144	2.62555	99.84
T2	43259.21709	0.03089	280.92310	0.00095	2.62650	99.88
Mf	1180292.34400	0.03074	17.46738	0.00095	2.62745	99.92
P1	86637.20483	0.02350	263.22070	0.00055	2.62800	99.94
lambda2	43998.38690	0.01892	247.25226	0.00036	2.62836	99.95
M8	11178.54108	0.01765	353.72296	0.00031	2.62867	99.96
Q1	96726.08376	0.01580	233.09831	0.00025	2.62892	99.97
MKS2	44587.80812	0.01391	75.78927	0.00019	2.62911	99.98
Ssa	15778463.36000	0.01165	359.24103	0.00014	2.62925	99.99
N4	22785.02679	0.00983	53.53183	0.00010	2.62935	99.99
S1	86399.98873	0.00846	184.02820	0.00007	2.62942	99.99
S4	21600.00000	0.00806	193.05556	0.00006	2.62948	99.99
M3	29809.44289	0.00645	164.86276	0.00004	2.62952	100.00
Mtm	789085.41440	0.00632	12.12263	0.00004	2.62956	100.00
MNS2	47258.16272	0.00627	259.93463	0.00004	2.62960	100.00
R2	43140.94484	0.00421	280.40744	0.00002	2.62962	100.00
Sa	31556955.92000	0.00298	352.87988	0.00001	2.62963	100.00
J1	83154.51628	0.00139	334.46280	0.00000	2.62963	100.00

Source: FES (2014).

Semidiurnal tidal constituents predominantly control tidal dynamics. Among them, the M2 constituent (principal lunar semidiurnal) plays a dominant role, accounting for up to 86.5% of tidal variability. In combination with the S2 (principal solar semidiurnal), N2 (larger lunar

elliptic semidiurnal), and K1 (luni-solar diurnal) constituents, these components explain more than 85% of the semidiurnal tidal signal, as reported by Foreman (1977) (Table 2).

According to Foreman (1977), tidal regimes at a given location can be temporally characterized using the form number (*F*) proposed by Dietrich (1963). This parameter is calculated from the ratio of the amplitudes of the principal harmonic constituents M2, S2, K1, and O1, as defined by the equation presented in Table 2. Based on the occurrence of High Tide (HT) and Low Tide (LT) during a lunar day (24 h 50 min), tides are classified as semidiurnal, diurnal, or mixed. Semidiurnal tides are characterized by two HTs and two LTs per lunar day, whereas diurnal tides exhibit only one HT and one LT within the same period. Mixed tides display both semidiurnal and diurnal characteristics, resulting in significant height differences between successive HTs or LTs. Under this regime, two HTs and two LTs typically occur each day; however, episodic transitions to a diurnal pattern may occur (Nascimento and Silva, 2019).

Table 2

Form number using amplitude value of some harmonic constants (Dietrick, 1963; Foreman, 1977).

$F = \frac{\mathrm{K1-O1}}{\mathrm{M2-S2}}$	The tide is then said to be: (i)semidiurnal if 0 ≤ F ≤ 0.25, (iii) mixed mostly semidiurnal if 0.25 < F ≤ 3.00, (iii) mixed mostly diurnal if 0.25 < F ≤ 3.00, (iv) diurnal if F > 3.00

Source: Foreman (1977).

According to its propagation characteristics, tidal waves can be classified as stationary, progressive, or mixed. A tidal wave exhibits stationary (or standing) behavior when the travel time to and from the head of the estuary is equal to the tidal period. A stationary wave is further characterized by a phase lag where maximum velocities coincide with the mean water level (mid-flood and mid-ebb), while the lowest velocities – close to zero – occur during High Tide (HT) and Low Tide (LT), representing the slack water periods (Dyer, 1986).

Conversely, a progressive tidal wave occurs when its energy is completely dissipated by friction before reflection. In this case, maximum currents and velocities occur at HT and

LT. Consequently, the slack water periods are lagged by 90 degrees relative to HT and LT; that is, minimum velocities occur at the mean tidal levels.

The mixed tide is a composition of both progressive and stationary waves. In estuarine environments, the tidal wave amplitude tends to increase upstream due to narrowing (funneling); however, it eventually decreases due to energy dissipation by bottom friction or wave reflection (Dyer, 1986).

- River Discharge Data

The river discharge data for the water bodies included in the modeling were estimated based on characteristic average flow velocities for the region (UA, 2019) and the cross-sectional dimensions of the Guamá, Moju, Acará, Tocantins, and Pará rivers at the boundary sections of the modeling domain. These estimates also incorporate the bathymetry adopted for the boundary reaches of the aforementioned water bodies to ensure accurate volume flux calculations.

3 RESULTS AND DISCUSSION

This section presents and discusses the results obtained in the simulations.

3.1 HYDRODYNAMIC CHARACTERISTICS

Hydrodynamic circulation in Marajó Bay primarily depends on astronomical tides, bathymetry, bottom roughness, wind patterns, and the fluvial discharge of its tributaries. In the study area, Marajó Bay has an average depth of 9.33 m. The bay extends in a NE-SW direction, spanning approximately 204 km between the open boundary and the head of the estuary (the farthest point on the river boundary). Its width measures 50 km at the mouth, narrowing to 14 km in the area influenced by the Barcarena Industrial District (DIB).

Based on its bathymetric characteristics, the Marajó Bay system can be classified as a coastal plain estuary. It features fluvial plains in areas under significant tributary influence, exhibiting a topography similar to a river valley. The system is relatively shallow, with depths rarely exceeding 30 m, and its cross-section broadens progressively toward the mouth.

3.2 CIRCULATION PATTERNS AND CURRENT VELOCITIES

The results of the hydrodynamic modeling regarding circulation patterns and current velocities are presented below.

Average tidal current velocities recorded at three stations distributed throughout the study area ranged between 0.40 and 0.49 m/s during the rainy season, and 0.37 to 0.48 m/s during the dry season. Maximum current velocities reached 1.1 m/s in both seasonal periods (Table 3). These velocities are influenced by bathymetry and equivalent bottom roughness, which also affect tidal amplitude and phase propagation.

Table 3

Comparison of depth-averaged current velocities across the selected monitoring stations.

Item	**Average speed in the rainy season**			**Average speed in the dry season**		
Stations	Boca	Vila do Conde	R. Tocantins-M	Boca	Vila do Conde	R. Tocantins-M
Media Speed - m/s	0.40	0.48	0.49	0.37	0.48	0.40
Maximum Speed - m/s	1.10	0.92	0.91	0.99	0.99	1.10

Source: Prepared by the authors themselves.

The time series recorded at the stations of Boca da Baía, situated at the open boundary, and Rio Tocantins Montante, located at the fluvial boundary of the model, exhibited two similar tidal cycles per lunar day. This pattern is characteristic of a semidiurnal tide regime, as defined by Dyer (1986) (Figures 4 and 5).

This tidal classification was further corroborated by the calculated Form Factor (F), derived from the harmonic constants. The analysis yielded a value of 0.10, falling within the range of $0 \leq F \leq 0.25$, which is the characteristic interval for semidiurnal tides according to Dietrich (1963).

Figure 4

Tidal elevation time series at the Boca da Baía and Rio Tocantins Montante stations during the rainy season.

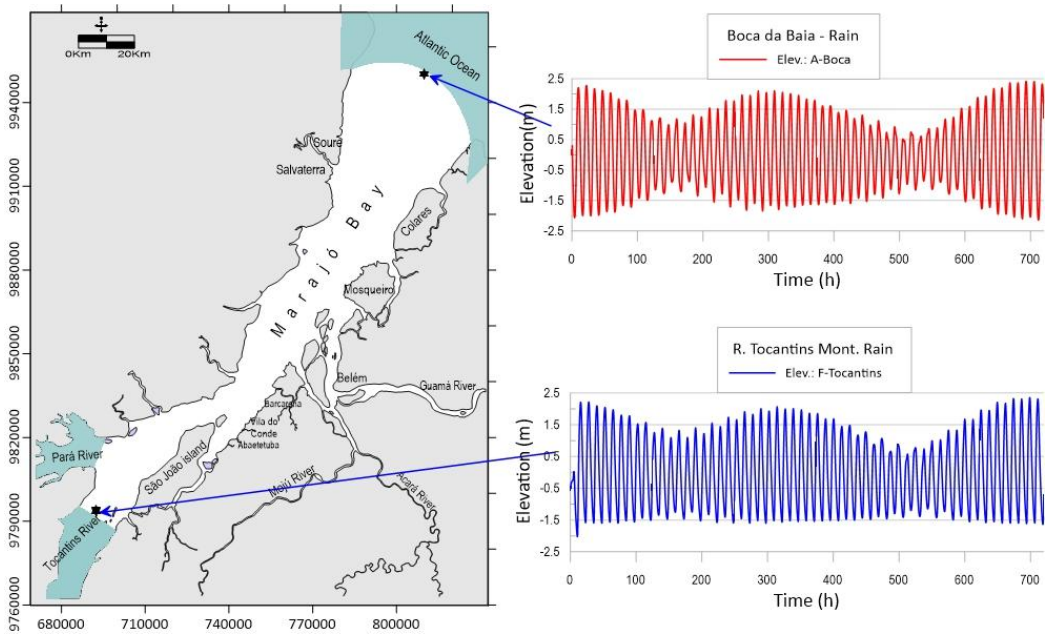

Source: Prepared by the authors themselves.

Figure 5

Tidal signal at the Boca da Baía and Rio Tocantins Montante stations during the dry season.

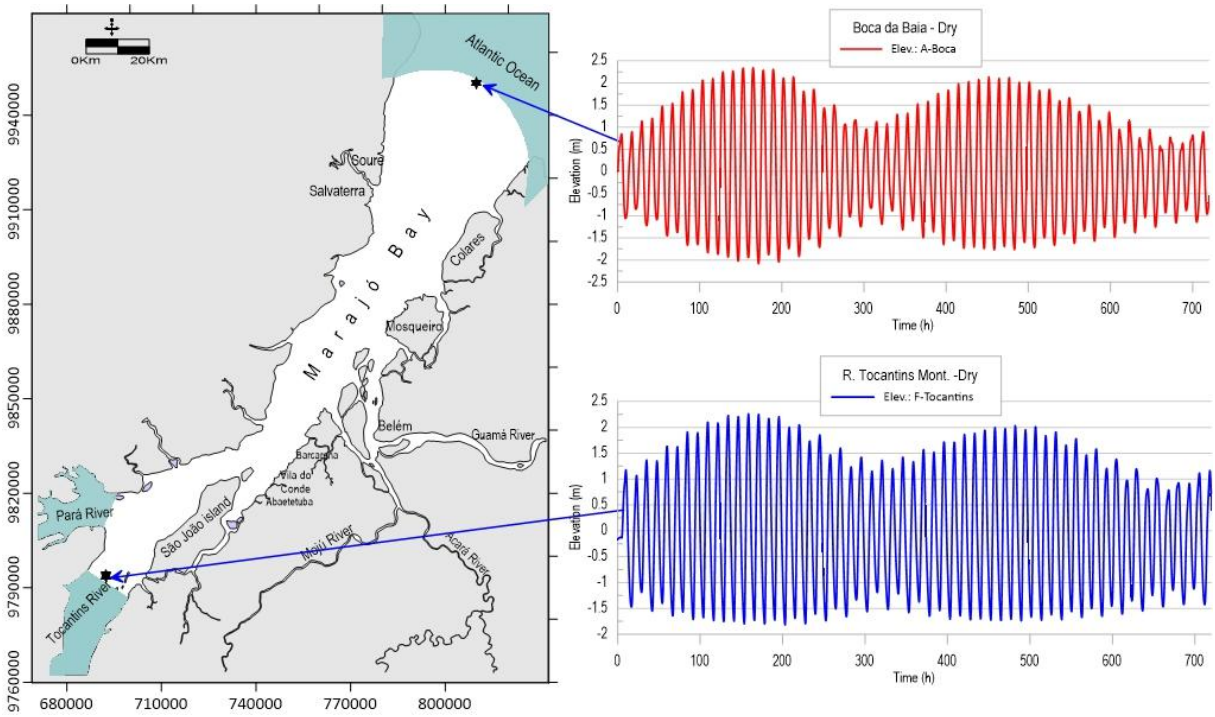

Source: Prepared by the authors themselves.

According to Foreman (1977), semidiurnal tides are predominantly influenced by the harmonic constants M2 (principal lunar), S2 (principal solar), N2 (larger lunar elliptic), and K2 (luni-solar semidiurnal), which together account for 85% or more of the total tidal elevation variance. In Marajó Bay, these constituents are responsible for 97.65% of the tidal behavior (Table 1).

Figures 6 and 7 illustrate the tidal wave propagation at the Boca da Baía and Rio Tocantins Montante stations during the rainy and dry seasons, respectively. The results indicate that Marajó Bay exhibits a mixed tidal behavior with a strong stationary tendency. This is evidenced by the fact that the flood slack water (EEn) and ebb slack water (EVz) closely coincide with High Tide (HT) and Low Tide (LT).

Accordingly, the maximum current velocities during flood and ebb cycles occurred during mid-flood and mid-ebb (at the mean water level). An exception was observed at the Boca da Baía station, where the maximum current velocities were recorded closer to HT and LT, suggesting a more progressive wave behavior at the mouth of the bay.

Figure 6

Tidal signal during the rainy season at stations: (a) Boca da Baía and (b) Rio Tocantins Montante.

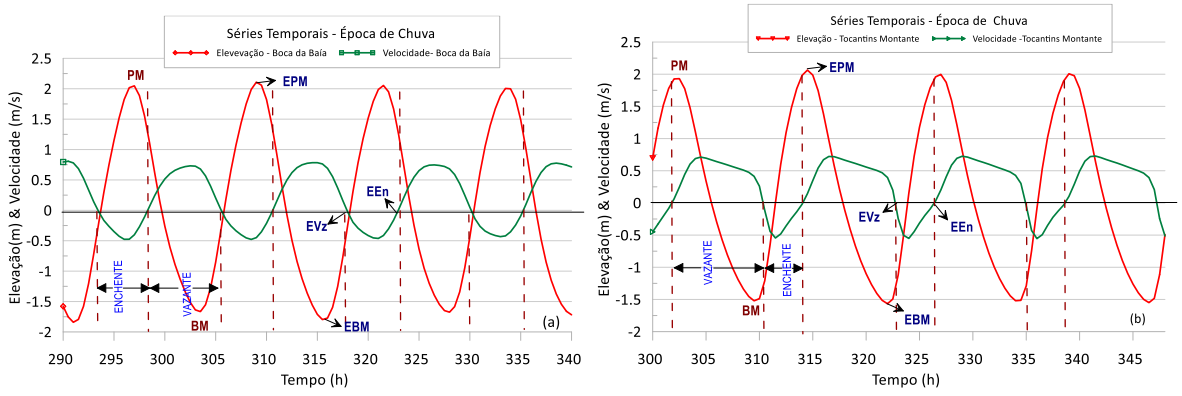

HT = High Tide; **LT** = Low Tide; **SHT** = Slack High Tide (Estofa de Preamar); **SLT** = Slack Low Tide (Estofa de Baixamar); **ES** = Ebb Slack (Estofa de Vazante); **FS** = Flood Slack (Estofa de Enchente).
Source: Prepared by the authors themselves.

Figure 7

Tidal signal during the dry season at stations: (a) Boca da Baía and (b) Rio Tocantins Montante.

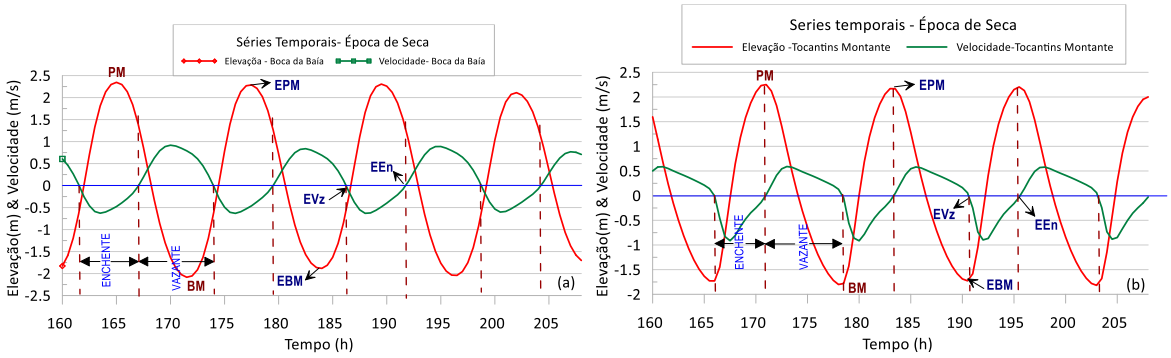

Source: Prepared by the authors themselves.

Significant differences were observed between the durations of the flood and ebb cycles at both analyzed stations, with the ebb phase lasting longer than the flood phase. During the rainy season, the ebb duration accounted for 59% of the tidal cycle at the Boca da Baía station and 70% at the Rio Tocantins Montante station (Table 4).

These discrepancies can be attributed to the stronger influence of river discharge at the Rio Tocantins Montante station, contrasted with the greater oceanic influence at the Boca da Baía station. This same pattern of ebb dominance was observed during the dry season at both stations, although there was a slight decrease in ebb duration and a corresponding proportional increase in flood duration (Figures 6 and 7).

Table 4

Quantitative data of the mara in the two seasons evaluated in the dry and rainy season.

Average Time/Station	RAINY SEASON		DRY SEASON	
	R. Tocantins Montante	Boca da Baia	R. Tocantins Montante	Boca da Baia
Duration of the Ebb - h	8.59	7.24	7.39	6.89
Duration of Flood - h	3.67	5.02	4.98	5.51
Total tidal cycle - h	12.26	12.26	12.37	12.40
% of time leaking	70.09	59.05	59.73	55.58
% of time filling	29.91	40.95	40.27	44.42

Source: Prepared by the authors themselves.

In quantitative terms, during the dry season, the ebb phase persisted for 55.6% of the cycle at the Boca da Baía station and 59.7% at the Rio Tocantins Montante station. These variations are likely driven by the significant reduction in river discharge from the tributaries

of Marajó Bay (Table 4). Studies by Santos (2014) indicate that at locations near the open boundary, the ebb duration accounted for 53% of the tidal cycle, increasing progressively toward the head of the estuary, where the ebb reached 60% of the total cycle.

The propagation of the tidal wave along the bay is illustrated in Figure 8, which presents the elevation time series at three reference stations to estimate the tidal phase lag. The distances from the Boca da Baía station are approximately 78 km to the Mosqueiro station and 204 km to the Rio Tocantins Montante station.

The recorded phase lag for the High Tide (HT) instant was 1.8 hours between Mosqueiro and Boca da Baía, and 5.5 hours between Rio Tocantins Montante and Boca da Baía. These data indicate that the tidal wave propagates with a phase lag of approximately 1 hour every 40 km. This velocity is influenced by bathymetry, bottom roughness, the morphology of the margins, and the sinuosity of the water bodies within the estuarine system.

Figure 8

Tide in the rainy season in the stations Boca da Baia, Mosqueiro and Rio Tocantins Montante.

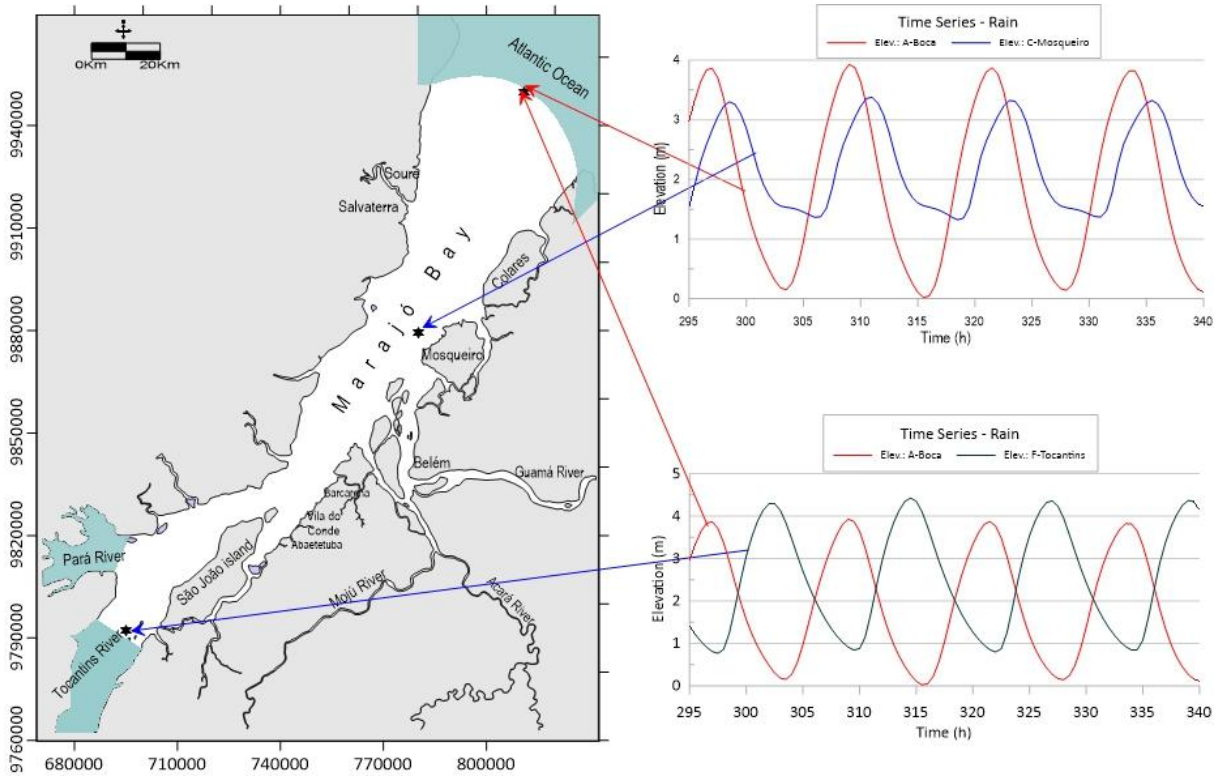

Source: Prepared by the authors themselves.

The vertical tidal movements in Marajó Bay are primarily driven by the gravitational attraction of the Moon and the Sun. When these forces align, they produce the highest

elevations, known as spring tides (syzygy). Conversely, the lowest elevations, or neap tides (quadrature), occur when the alignment of these celestial bodies forms a 90° angle. Spring and neap cycles occur twice during each lunation – the 29.53 – day interval between successive lunar conjunctions or oppositions.

Figures 9 and 10 illustrate the tidal behavior across both monthly and 24-hour scales at the Rio Tocantins Montante and Boca da Baía stations. These figures demonstrate how flow directions, current velocities, and the durations of flood and ebb phases shift during March (rainy season) and October (dry season). Intervals of approximately 14.7 days were observed between subsequent spring and neap tide events.

Figure 9

Illustrates the tidal behavior during the rainy season (March 2021) at the Rio Tocantins Montante station, highlighting the elevation fluctuations between spring (syzygy) and neap (quadrature) tides over a 30-day period.

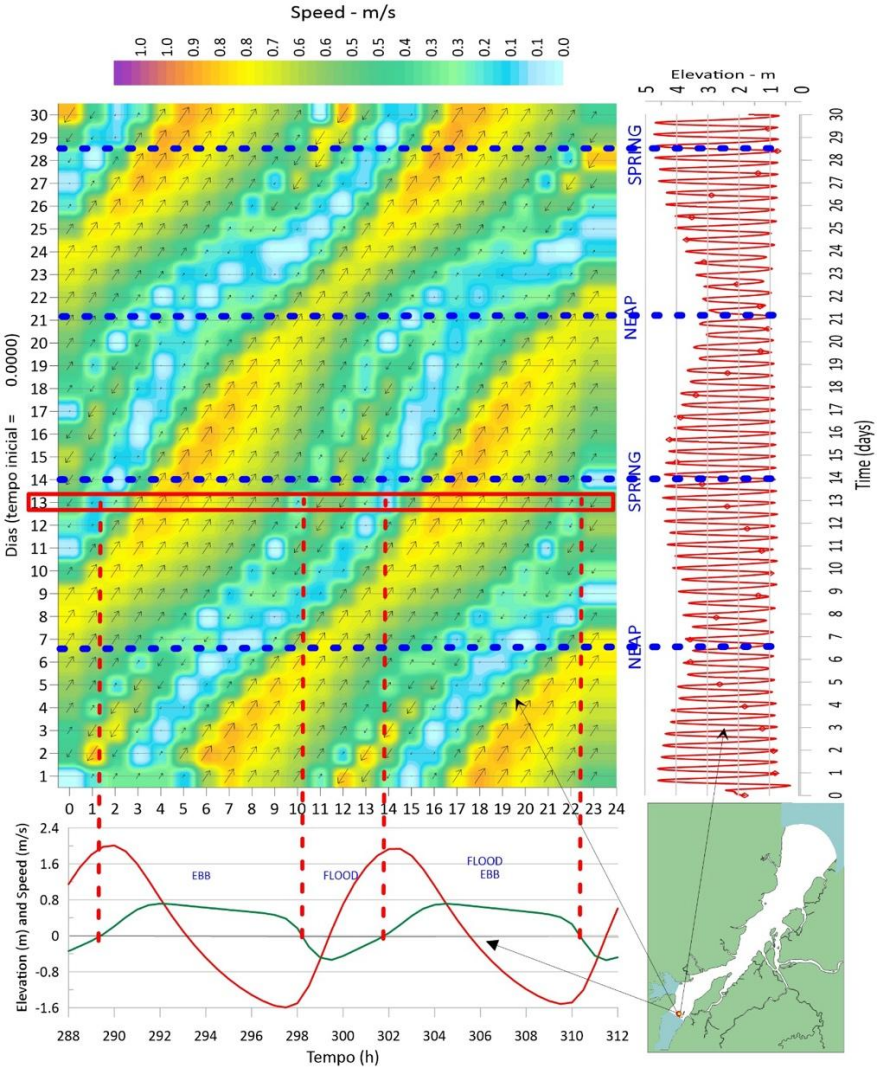

Source: Prepared by the authors themselves.

Figure 10

Tidal signal during the rainy season (March 2021) at the Boca da Baía station: (a) 30-day elevation series highlighting spring (syzygy) and neap (quadrature) cycles, and (b) flood and ebb phase durations for March 13, 2021.

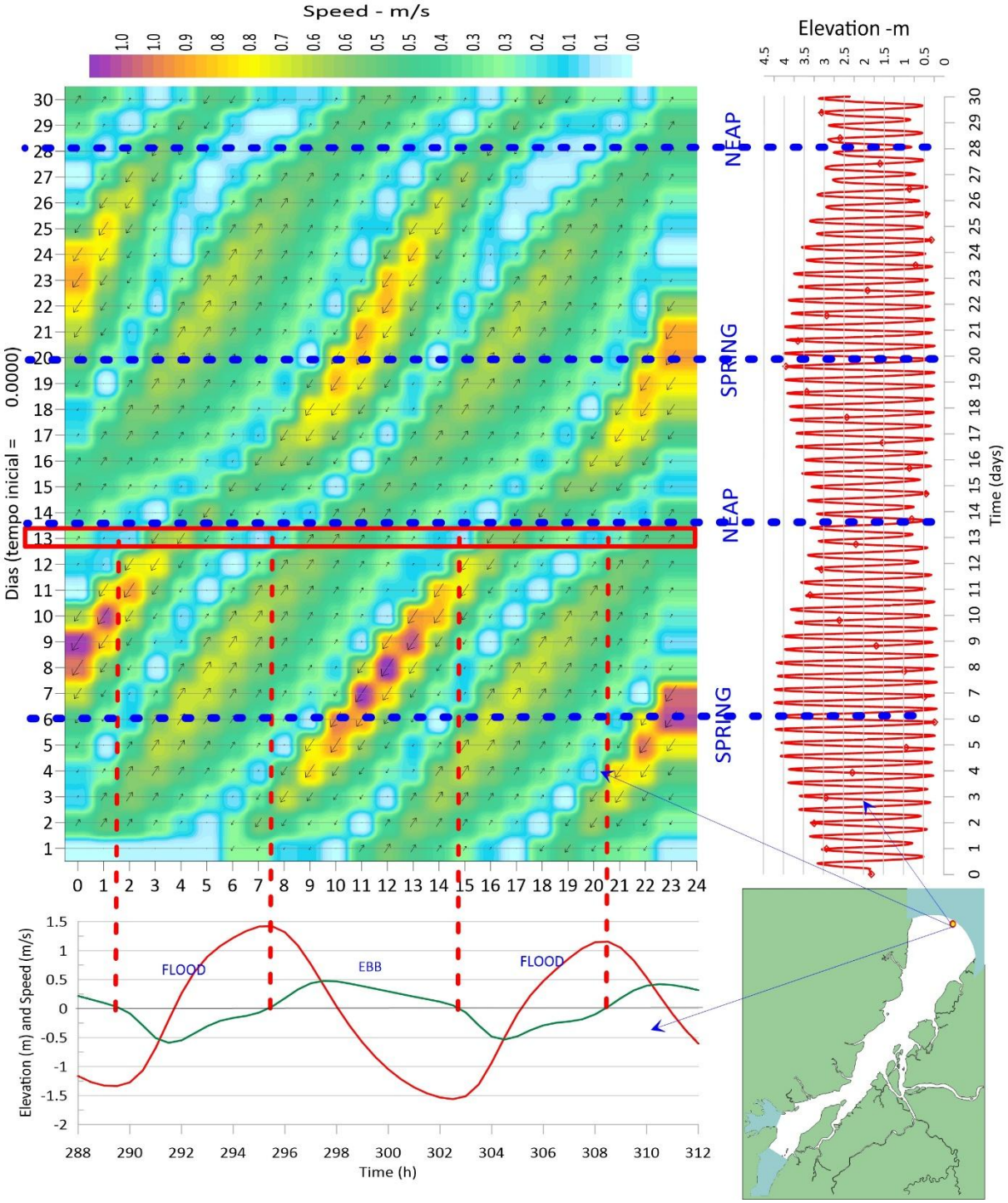

Source: Prepared by the authors themselves.

The Boca da Baía station recorded maximum velocities following the ebb phase of the spring tide, reaching up to 1.04 m/s. This value is slightly higher than those recorded at the Rio Tocantins Montante station, which reached 0.9 m/s under similar conditions.

The highest velocities in the rainy season occur during the ebb, near spring tide conditions and shortly after High Tide (HT). A time lag of approximately 50 minutes between subsequent high and low tides was observed, resulting from the lunar day duration (24 h 50 min). This lag generates a progressive shift in tidal characteristics throughout the month, creating the diagonal pattern (approximately 45°) observed in Figure 9.

Figures 9 and 10 demonstrate that at the Rio Tocantins Montante station, the ebb slack (EVz) occurs shortly after Low Tide (LT), while the flood slack (EEn) occurs just before High Tide (HT). This behavior differs from the Boca da Baía station, where EVz and EEn are recorded immediately following LT and HT, respectively. Notable differences in current velocities were observed between the two stations at the boundaries of the study area: at the Boca da Baía station, peak velocities occur just before HT and LT, whereas at the Tocantins station, the highest speeds are reached near the mid-flood and mid-ebb (mean water level). These phase relationships between slack water timing and velocity peaks are characteristic of a standing wave (stationary tide), which is predominant in Marajó Bay. Furthermore, the figures reveal two stationary cycles per lunar day, with the ebb phase consistently outlasting the flood phase in both seasons. This asymmetry is driven by the significant river discharge at the Tocantins station, contrasted with the dominant oceanic forcing at the Boca da Baía station.

To determine the water level variations in Marajó Bay, spring (syzygy) and neap (quadrature) tides during the rainy season were used to generate elevation maps. The Rio Tocantins Montante station was taken as a reference to illustrate tidal peaks. During this season, the highest elevations were recorded during spring High Tide (HT), with a tidal range of 3.6 m, contrasting with the lower range of 1.75 m recorded during neap HT (Table 5 and Figures 11 and 12).

The 204 km distance between the open boundary and the head of the estuary (fluvial boundary) results in significant spatio-temporal variations in tidal propagation along the bay. When the open boundary reaches HT, the head of the estuary simultaneously records elevations characteristic of Low Tide (LT), with intermediate gradients distributed across the study area, as shown in the spatial snapshots in Figures 11 and 12.

Figure 11

Tidal elevation in Marajó Bay during spring tide (syzygy) in the rainy season, referenced by the Rio Tocantins Montante station: (a) High Tide (HT) and (b) Low Tide (LT).

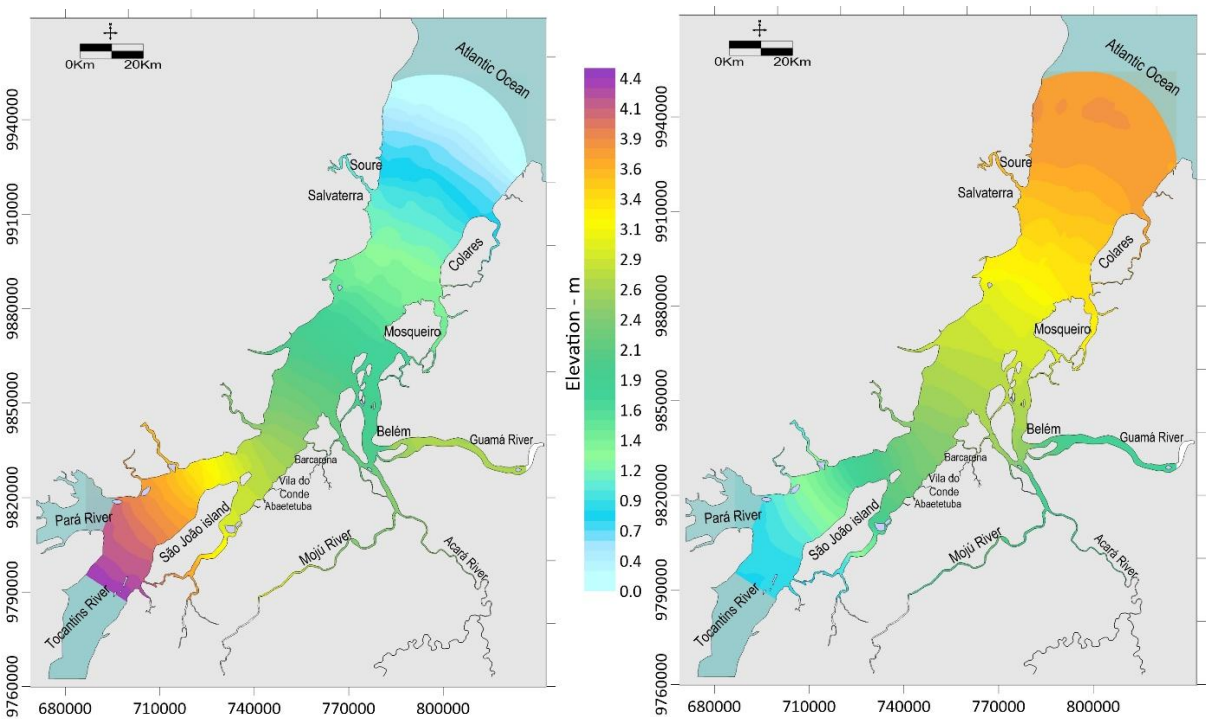

Source: Prepared by the authors themselves.

Table 5

Tidal elevation data during spring (syzygy) and neap (quadrature) cycles at the Rio Tocantins Montante station (Rainy Season – March 2021).

Type	State	Hours	Days	Elevation - m	Amplitude-m
Syzygy during the rainy season	PM	315,0	13.12	4.35	3.56
	BM	322,0	13.41	0.79	
Squareness during the dry season	PM	667,0	27.79	2.64	1.81
	BM	673,0	28.04	0.83	

Source: Prepared by the authors themselves.

Figure 12

Tidal elevation in Marajó Bay during neap tide (quadrature) in the dry season, referenced by the Rio Tocantins Montante station: (a) High Tide (HT) and (b) Low Tide (LT).

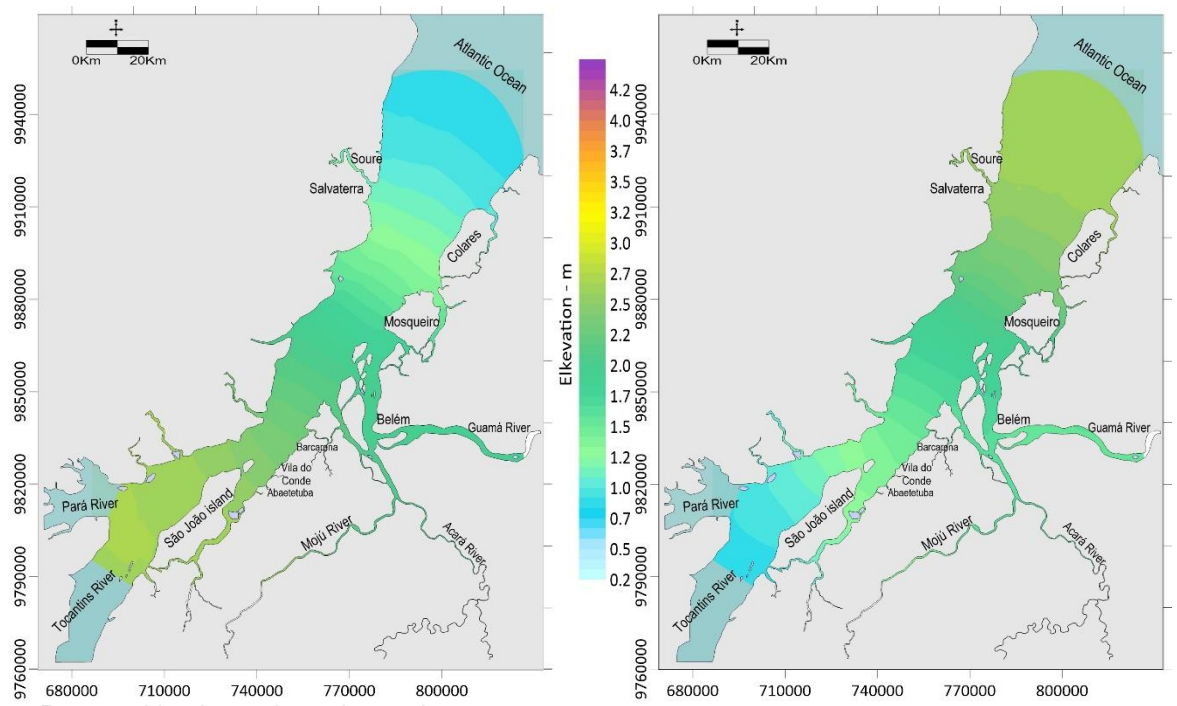

Source: Prepared by the authors themselves.

4 FINAL CONSIDERATIONS

The results of the Hydrodynamic Circulation Modeling conducted for the Pará River system, including Guajará and Marajó Bays, demonstrate that the water level undergoes two distinct ebb and flood cycles per lunar day. The calculated Form Number (F) remains within the range of $0 \leq F \leq 0.25$, which is characteristic of a semidiurnal tidal regime.

Based on the analysis of vertical elevation and horizontal velocity components, the results indicate that the study area is predominantly governed by a mixed standing tide (stationary behavior). The most influential astronomical constituents in the system are the semidiurnal components M_2 (principal lunar), S_2 (principal solar), N_2 (larger lunar elliptic), and K_2 (luni-solar semidiurnal), which together account for 97.6% of the tidal variance.

Tidal propagation across the modeling domain exhibits wave symmetry in areas near the open boundary. In contrast, significant tidal asymmetry is observed within the interior of the domain, particularly in the upstream reaches of the Guamá, Acará, Moju, Pará, and Tocantins rivers, where fluvial discharge and bottom friction further distort the tidal wave.

Significant differences were recorded in the durations of the flood and ebb phases at both analyzed stations. Overall, the ebb duration exceeds that of the flood, characterizing a

regime of ebb dominance. During the rainy season, the ebb phase accounted for 59% of the tidal cycle at the Boca da Baía station and 70% at the Rio Tocantins Montante station. In the dry season, the ebb persisted for 65% of the time at Boca da Baía, whereas at the Rio Tocantins Montante station, it decreased to 45%, indicating a seasonal shift toward flood dominance at this location.

It was observed that the ebb duration generally increases with distance from the open boundary toward the interior of the system. This phenomenon is driven by the significant influence of river discharge from the tributaries of Marajó Bay, which opposes the tidal wave propagation and prolongs the receding flow.

The highest current velocities in both the rainy and dry seasons occur during the ebb phase near spring tide (syzygy), shortly after High Tide (HT). A consistent phase lag of approximately 50 minutes between subsequent HT and LT was observed, resulting from the duration of the lunar day.

The depth-averaged tidal current velocities, recorded across three stations within the hydrodynamic model, ranged from 0.40 to 0.49 m/s during the rainy season and from 0.37 to 0.48 m/s during the dry season.

The maximum current velocity reached 1.1 m/s across both simulated periods. The data indicate a phase lag in tidal propagation of approximately 1 hour every 40 km, a value influenced by bathymetry, bottom roughness, coastal morphology, and the sinuosity of the estuarine channels.

These preliminary results for Marajó Bay are consistent with the hydrodynamics of equatorial estuarine systems, where semidiurnal tides and standing wave propagation predominate.

ACKNOWLEDGES

To the University of the State of Pará (UEPA) and the Federal Institute of Education, Science, and Technology of Pará (IFPA) for granting the necessary leave to pursue these postdoctoral studies. To the Graduate Program in Ocean Engineering (PENN/COPPE) at the Federal University of Rio de Janeiro (UFRJ) for the opportunity and acceptance into their distinguished research program;

To the Center for Natural Sciences and Technology (CCNT/UEPA) for providing the faculty development scholarship, supporting both the Undergraduate Environmental Engineering

program and the Graduate Program in Environmental Sciences (Master's and Doctorate levels);

To Dr. Paulo Rosman, Professor at the Graduate Program in Ocean Engineering (COPPE/UFRJ) and postdoctoral supervisor, for his invaluable teachings, patience, and expert guidance throughout this research.

REFERENCES

BARROS, M. L. C. **Modelagem hidrodinâmica e de qualidade de água em corpos de água com alagamento e secamento**. 2012. Thesis (PhD in Ocean Engineering) – Instituto Alberto Luiz Coimbra de Pós-Graduação e Pesquisa de Engenharia (COPPE), Universidade Federal do Rio de Janeiro, Rio de Janeiro, 2012. https://coc.ufrj.br/lista-teses-de-doutorado/modelagem-hidrodinamica-e-de-qualidade-de-agua-em-corpos-de-agua-com-alagamento-e-secamento/

CASTRO, E. R.; CARMO, E. D. Desastres e crimes da mineração em Barcarena, Mariana e Brumadinho na perspectiva da ecologia política e das comunidades locais. *In*: CASTRO, E. R.; CARMO, E. D. (eds.). **DOSSIÊ desastres e crimes da mineração em Barcarena**. Belém: NAEA: UFPA, 2019.

COMPANHIA DE DESENVOLVIMENTO ECONÔMICO DO PARÁ (Codec). Barcarena. **Codec**, Belém, nov. 2018. Available at: http://www.codec.pa.gov.br/barcarena#afooter. Access: 2018, Nov. 09.

CONAMA (Brasil). Resolução n° 357, de 17 de março de 2005. Dispõe sobre a classificação dos corpos de água e diretrizes ambientais para o seu enquadramento, bem como estabelece as condições e padrões de lançamento de efluentes, e dá outras providências. **Diário Oficial [da] União**: seção 1, Brasília, DF, n. 053, p. 58-63, 18 mar. 2005.

CONAMA (Brasil). Resolução n° 430, de 13 de maio de 2011. Dispõe sobre as condições e padrões de lançamento de efluentes, complementa e altera a Resolução no 357, de 17 de março de 2005, do Conselho Nacional do Meio Ambiente-CONAMA. **Diário Oficial [da] União**: seção 1, Brasília, DF, n. 92, p. 89, 16 maio. 2011.

DIETRICH, G. **General Oceanography**. New York: Interscience Publishers, 1963.

DYER, K. R. **Coastal and estuarine sediment dynamics**. Chichester, UK: John Wiley & Sons, 1986.

FES 2014. FINITE ELEMENT SOLUTION (FES). Tide model released. Disponível em: https://datastore.cls.fr/catalogues/fes2014-tide-model/. Acesso em 22/11/2022.

FOREMAN, M. G. G. **Manual for Tidal Heights Analysis and Prediction**. **Pacific Marine Science Report 77-10**. Patricia Bay, BC: Institute of Ocean Sciences, 1977.

GALLO, M. N. **Escoamento em planícies de maré com influência fluvial – Canal Norte do Rio Amazonas**. 2009. Thesis (PhD in Ocean Engineering) – Instituto Alberto Luiz Coimbra de Pós-Graduação e Pesquisa de Engenharia (COPPE), Universidade Federal do Rio de Janeiro. Rio de Janeiro, 2009. https://oceanica.ufrj.br/thesis/2009

IEC (Brasil). Relatório Técnico 03/2018. Avaliação preliminar dos impactos ambientais referente ao transbordo e lançamentos irregulares de efluentes de lama vermelha na cidade de Barcarena, estado do Pará. **Instituto Evandro Chagas**: relatório 003, Ananindeua, PA, p. 1-51, 28 mar. 2018.

LIMA NETO, I. E. *et al*. Simulação da compartimentação em reservatório no semiárido brasileiro uso da modelagem hidrodinâmica como ferramenta de gestão. **Revista DAE**, São Paulo, v. 69, n. 231, p. 41-53, jul./set. 2021. https://doi.org/10.36659/dae.2021.045.

NASCIMENTO, P. A. M.; SILVA, H. P. Saúde ambiental e impactos da mineração em Barcarena, Pará, Brasil: o caso da Comunidade Bom Futuro. *In*: MIRANDA, A. M. M. (eds.) **Pesquisa em saúde e ambiente no ambiente na Amazônia**: perspectivas para sustentabilidade humana e ambiental na região. Guarujá, SP: 2021. http://dx.doi.org/10.37885/210504445.

PEREIRA, S. F. *et al*. Estudo químico ambiental do rio Murucupi – Barcarena, PA, Brasil, área impactada pela produção de alumínio. **Revista AmbiÁgua**, Taubaté, v. 2, n. 3, p. 62-82, 2007. http://dx.doi.org/10.4136/ambi-agua.34

ROSMAN, P. C. C. Modelagem de hidrodinâmica ambiental, qualidade de água e processos sedimentológicos em rios conexos à UHE estreito. Fundação COPPETEC - **Projeto PENO-10702 com CESTE** - Consórcio Estreito Energia, Rio de Janeiro, 2012.

ROSMAN, P. C. C. (ed.). **Referência Técnica do SisBahia - Sistema Base de Hidrodinâmica Ambiental**. Rio de Janeiro: COPPE/UFRJ, 2013. Available at: http://www.sisbahia.coppe.ufrj.br/ SisBAHIA_RefTec_V9d_.pdf . Access: 2021, Apr. 05.

UNIVERSO AMAZÔNIA CONSULTORIA E ANÁLISES AMBIENTAIS LTDA (UA). **Estudos hidrológicos para o lançamento do efluente industrial do Polo Acará da Biopalma no Rio Acará**. Belém: Biopalma S.A., 2019.